CHEMISTRY
A EUROPEAN JOURNAL

DOI: 10.1002/chem.200600409

Crystal Structure, Physical Properties and HRTEM Investigation of the New Oxonitridosilicate $EuSi_2O_2N_2$

Florian Stadler,[a] Oliver Oeckler,[a] Henning A. Höppe,[a, b] Manfred H. Möller,[c] Rainer Pöttgen,[c] Bernd D. Mosel,[d] Peter Schmidt,[e] Viola Duppel,[f] Arndt Simon,[f] and Wolfgang Schnick*[a]

Abstract: The new layered oxonitridosilicate $EuSi_2O_2N_2$ has been synthesized in a radio-frequency furnace at temperatures of about 1400 °C starting from europium(III) oxide (Eu_2O_3) and silicon diimide ($Si(NH)_2$). The structure of the yellow material has been determined by single-crystal X-ray diffraction analysis (space group $P1$ (no. 1), $a = 709.5(1)$, $b = 724.6(1)$, $c = 725.6(1)$ pm, $\alpha = 88.69(2)$, $\beta = 84.77(2)$, $\gamma = 75.84(2)°$, $V = 360.19(9) \times 10^6$ pm^3, $Z = 4$, $R1 = 0.0631$, 4551 independent reflections, 175 parameters). Its anionic $Si_2O_2N_2^{2-}$ layers consist of corner-sharing $SiON_3$ tetrahedra with threefold connecting nitrogen and terminal oxygen atoms. High-resolution transmission electron micrographs indicate both ordered and disordered crystallites as well as twinning. Magnetic susceptibility measurements of $EuSi_2O_2N_2$ exhibit Curie–Weiss behavior above 20 K with an effective magnetic moment of 7.80(5) μ_B Eu^{-1}, indicating divalent europium. Antiferromagnetic ordering is detected at 4.5(2) K. $EuSi_2O_2N_2$ shows a field-induced transition with a critical field of 0.50(5) T. The four crystallographically different europium sites cannot be distinguished by ^{151}Eu Mössbauer spectroscopy. The room-temperature spectrum is fitted by one signal at an isomer shift of $\delta = -12.3(1)$ mm s^{-1} subject to quadrupole splitting of $\Delta E_Q = -2.3(1)$ mm s^{-1} and an asymmetry parameter of 0.46(3). Luminescence measurements show a narrow emission band with regard to the four crystallographic europium sites with an emission maximum at $\lambda = 575$ nm.

Keywords: electron microscopy · luminescence · magnetic properties · oxonitridosilicates · structure elucidation

[a] Dipl.-Chem. F. Stadler, Dr. O. Oeckler, Dr. H. A. Höppe, Prof. Dr. W. Schnick
Department Chemie und Biochemie
Lehrstuhl für Anorganische Festkörperchemie
Ludwig-Maximilians-Universität München
Butenandtstrasse 5–13 (D), 81377 München (Germany)
Fax: (+49) 89-2180-77440
E-mail: wolfgang.schnick@uni-muenchen.de

[b] Dr. H. A. Höppe
New address: Institut für Anorganische und Analytische Chemie
Albert-Ludwigs-Universität
Albertstrasse 21, 79104 Freiburg (Germany)

[c] Dr. M. H. Möller, Prof. Dr. R. Pöttgen
Institut für Anorganische und Analytische Chemie
Universität Münster
Corrensstrasse 30, 48149 Münster (Germany)

[d] Dr. B. D. Mosel
Institut für Physikalische Chemie, Universität Münster
Corrensstrasse 30/36, 48149 Münster (Germany)

[e] Dr. P. Schmidt
Philips Research Laboratories Aachen
Weisshausstrasse 2, 52066 Aachen (Germany)

[f] V. Duppel, Prof. Dr. A. Simon
Max-Planck-Institut für Festkörperforschung
Heisenbergstrasse 1, 70569 Stuttgart (Germany)

Introduction

Nitridosilicates extend the structural variety of the naturally occurring oxosilicates because nitrogen atoms can connect two, three, or even four silicon atoms to form highly condensed network structures.[1] Furthermore, edge-sharing of two tetrahedra to form a Si_2N_6 unit is possible in nitridosilicates.[2,3] Recently, we synthesized some new oxonitridosilicates that combine structural features and properties of both oxosilicates and nitridosilicates. For example, the calcium oxonitridosilicate $CaSi_2O_2N_2$ consists of corrugated layers of corner-sharing $SiON_3$ tetrahedra.[4]

These compounds (sions as well as sialons) gained significant relevance in materials science because of their remarkable chemical and thermal stability and they have been considered as host lattices for rare-earth-doped phosphors in light-emitting diode (LED) applications.[5] The rare-earth ions Eu^{2+} and Ce^{3+} are quite suitable because both show parity-allowed fast 5d–4f emissions and are stable up to very high excitation intensities. The Eu^{2+} ion supplies a narrow emission and is therefore preferred for 2- and 3-pc

(phosphor-converted)-LED applications. Accordingly, much effort has been directed towards syntheses of new materials for better devices. A promising method for the synthesis of nitridosilicates is the use of radio-frequency furnaces.[6] The reaction of silicon diimide with Eu_2O_3 or $SrCO_3$ powder yields the oxonitridosilicates $EuSi_2O_2N_2$ and $SrSi_2O_2N_2$, respectively. A solid solution series with formulae $Eu_xSr_{1-x}Si_2O_2N_2$ has been obtained for the whole range of $0 \le x \le 1$.[7]

Close to the Sr end member of the solid solution series $(Sr,Eu)Si_2O_2N_2$, the compound $SrSi_2O_2N_2$:Eu is an important and highly effective yellow-green phosphor for pc-LED applications.[5] The unequivocal crystallographic characterization of Sr-rich compounds in this system proved to be difficult. Therefore, we have investigated in detail the crystal structure of isotypic $EuSi_2O_2N_2$ in this contribution. The topology of the anionic framework in $EuSi_2O_2N_2$ can be compared with that of the only natural Si-O-N mineral sinoite (Si_2N_2O; orthorhombic, space group $Cmc2_1$) that has been found in the impact craters of meteorites.[8] In the case of the related calcium sion $CaSi_2O_2N_2$ a topotactic reaction of CaO with Si_2N_2O to obtain $CaSi_2O_2N_2$ has been carried out successfully.[9]

Abstract in German: *Das neue schichtartig aufgebaute Oxonitridosilicat $EuSi_2O_2N_2$ wurde in einem Hochfrequenzofen bei etwa 1400 °C aus Europium(III)-oxid (Eu_2O_3) und Siliciumdiimid ($Si(NH)_2$) hergestellt. Die Kristallstruktur der gelben Verbindung wurde mittels Einkristallröntgenstrukturanalyse bestimmt (Raumgruppe P1 (Nr. 1), $a = 709.5(1)$, $b = 724.6(1)$, $c = 725.6(1)$ pm, $\alpha = 88.69(2)$, $\beta = 84.77(2)$, $\gamma = 75.84(2)°$, $V = 360.19(9) \cdot 10^6$ pm^3, $Z = 4$, $R1 = 0.0631$, 4551 unabhängige Reflexe, 175 Parameter). Die anionischen $Si_2O_2N_2^{2-}$-Schichten bestehen aus eckenverknüpften $SiON_3$-Tetraedern mit dreifach verbrückendem Stickstoff und terminalem Sauerstoff. Hochauflösende Transmissionselektronenmikroskopie (HRTEM) zeigt sowohl geordnete als auch ungeordnete Kristallite sowie Verzwillingung. Messungen der magnetischen Suszeptibilität von $EuSi_2O_2N_2$ ergeben oberhalb von 20 K Curie-Weiss-Verhalten mit einem effektiven magnetischen Moment von 7.80(5) μ_B Eu^{-1}, welches auf zweiwertiges Europium hinweist. Bei 4.5(2) K wird antiferromagnetische Ordnung detektiert. $EuSi_2O_2N_2$ zeigt einen feldinduzierten Übergang mit einem kritischen Feld von 0.50(5) T. Die vier kristallographisch unterschiedlichen Europiumatome konnten durch ^{151}Eu-Mößbauer-Spektroskopie nicht unterschieden werden. Das Raumtemperaturspektrum konnte durch ein Signal bei einer Isomerenverschiebung von $\delta = -12.3(1)$ mm s^{-1} gemäß einer Quadrupolaufspaltung von $\Delta E_Q = -2.3(1)$ mm s^{-1} und einem Asymmetrieparameter von 0.46(3) angepasst werden. Lumineszenzmessungen zeigten eine bzgl. der vier kristallographischen Europiumlagen schmale Emissionsbande mit einem Maximum bei $\lambda = 575$ nm.*

Herein we discuss structural features issues and present magnetic properties and ^{151}Eu Mössbauer spectra of the new sion $EuSi_2O_2N_2$.

Results and Discussion

Diffraction patterns and twinning: From X-ray diffraction patterns of $EuSi_2O_2N_2$ single crystals a triclinic unit cell ($a = 709.5(1)$, $b = 724.6(1)$, $c = 725.6(1)$ pm, $\alpha = 88.69(2)$, $\beta = 84.77(2)$, $\gamma = 75.84(2)°$) can be derived, however, structure solutions and refinements yield remarkably disordered structure models and exhibit high residual electron densities in difference Fourier syntheses. Closer inspection of the diffraction patterns reveals diffuse streaks along [010]*, indicating some kind of stacking faults, as well as more or less pronounced additional reflections that cannot be indexed on the basis of the given unit cell.

As data from one single crystal are not necessarily representative for the whole (mainly microcrystalline) sample, electron diffraction patterns have been recorded for about 30 crystallites originating from a powder sample. Whereas some of them exhibit diffuse streaks, most show only sharp reflections. However, only for some crystallites tilting series of diffraction patterns could be indexed completely based on the above-mentioned unit cell from X-ray data (Figure 1a). Many crystallites indicate twinning according to a twin law (-100, $-\frac{1}{2}10$, $00-1$), corresponding to a 180° rotation around [010]* or [$\bar{1}$40], respectively (Figure 1b).

This kind of twinning by reticular pseudomerohedry is possible because $\alpha^* = 90.03(2)°$. Reflections with $h = 2n$ overlap completely, whereas layers (hkl) with $h = 2n+1$ show additional reflections from the other twin individual. Reflections from both domains together can be indexed with a monoclinic C-centered twin lattice with $a = 709$, $b = 2810$, $c = 726$ pm and $\beta = 95.2°$, however, this "supercell" is not real. A comparable kind of twinning is described in detail in reference [10]. The diffuse scattering observed in some crystallites (cf. Figure 1c) can be explained (at least in most cases) assuming small twin domains because only the reflections that do not overlap for both orientations become diffuse. Therefore, we can conclude that the diffuse scattering observed in the X-ray diffraction patterns does not result from intrinsic structural disorder, but from a large number of twin boundaries due to very small twin domains. As different crystals show a varying degree of diffuse intensity, the final structure determination was carried out using the crystal with the weakest diffuse streaks. These were neglected as they result only from a very small fraction of the otherwise ordered crystal volume and do not influence Bragg intensities significantly. However, additional Bragg reflections due to the twinning cannot be ignored.

Crystal structure: The structure was initially solved by direct methods neglecting the twinning. During the refinement, the twin law was taken into account and no split positions or other disorder remained. Also, the residual electron density

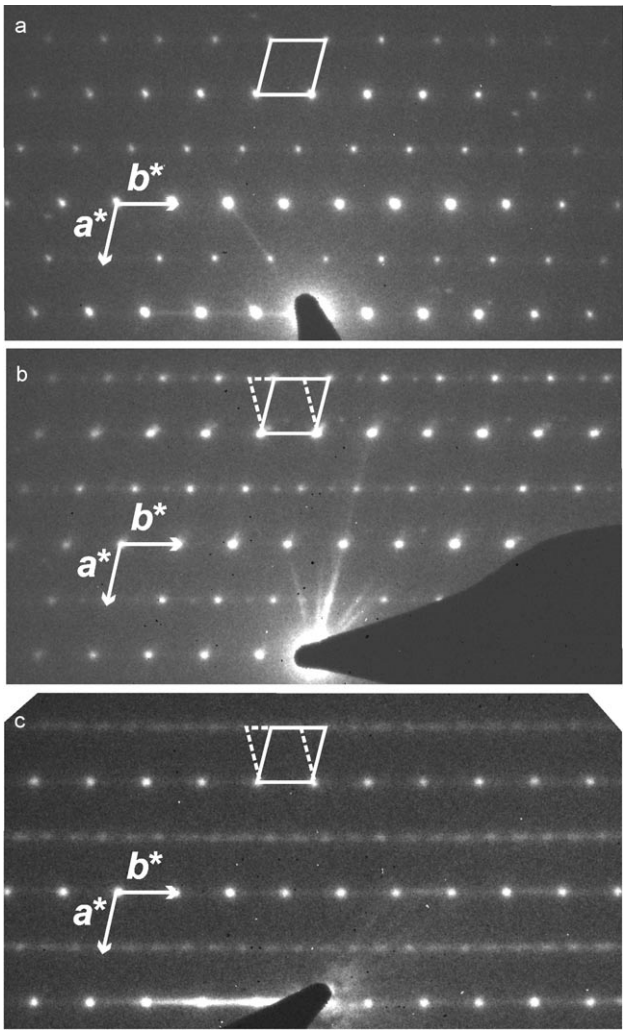

Figure 1. Electron diffraction patterns of different crystallites, zone axis [001]. a) The elementary mesh, b,c) the elementary mesh for both twin domain orientations is indicated.

Table 1. Crystal data of $EuSi_2O_2N_2$

formula	$EuSi_2O_2N_2$
formula weight [g mol^{-1}]	268.16
crystal system	triclinic
space group	$P\bar{1}$ (no. 1)
diffractometer type	STOE IPDS
radiation λ [pm]	71.073 (Mo-Kα)
crystal size [mm^3]	$0.185\times0.033\times0.026$
unit cell dimensions	
a [pm]	709.5(1)
b [pm]	724.6(1)
c [pm]	725.6(1)
α [°]	88.69(2)
β [°]	84.77(2)
γ [°]	75.84(2)
cell volume [10^6 pm^3]	360.19(9)
formula units Z	4
ρ_{calcd} [g cm^{-3}]	4.945
$F(000)$	484
μ [mm^{-1}]	17.906
temperature [K]	295(3)
θ range [°]	3.61–32.56
reflections	4551
observed reflections	3145 ($F_o^2 \geq 2\sigma(F_o^2)$)
absorption correction	semiempirical (from equivalents)
min./max. transmission	0.50/0.63
no. of refined parameters/restraints	175/3
min./max. $\Delta\rho_e$ [e Å^{-3}]	−2.306/2.272
Flack parameter	−0.06(3)
goodness of fit	0.919
$R1/wR2$ (all data)	0.0631/0.0839
$R1/wR2$ ($F_o^2 \geq 2\sigma(F_o^2)$)	0.0386/0.0777
weighting details	$w^{-1}=\sigma^2F_o^2 + (0.0462\ P)^2$; $P=[\mathrm{Max}(0,F_o^2) + 2\ F_c^2]/3$

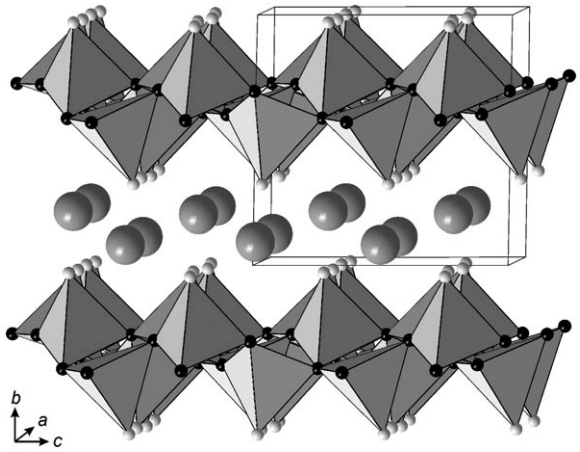

Figure 2. Crystal structure of $EuSi_2O_2N_2$, view along [100]. Eu large spheres, O light gray, N black. The $SiON_3$ tetrahedra as well as the unit cell are shown.

is satisfactorily low and is located near Eu atoms. Displacement parameters for Eu and Si atoms exhibit no unusual anisotropy. Details of the structure refinement are given in Table 1. Powder diffraction patterns calculated on the basis of the structure parameters obtained from the single-crystal data refinement fit well with the experimental powder pattern; a Rietveld refinement yields $wR_p = 0.053$.

The layered structure of $EuSi_2O_2N_2$ (Figure 2) consists exclusively of corner-sharing $SiON_3$ tetrahedra. All N atoms are shared between three neighboring tetrahedra ($N^{[3]}$), whereas each O atom is bonded terminally. Identical to the situation in $CaSi_2O_2N_2$[4] the molar ratio X:Si (X = O, N) is 2, which is unknown for a simple layer silicate within the group of oxosilicates, in which this molar ratio usually is indicative for a framework structure. This specific finding is due to the presence of $N^{[3]}$ atoms in the crystal structure of $EuSi_2O_2N_2$, which are surrounded by three Si atoms in an almost trigonal-planar arrangement (cf. Table 2). We expect that there is an ordering of the arrangement of O and N atoms in the structure, because threefold coordinated oxygen atomswould be rather more unusual than terminal bonding, and there is a clear differentiation between Si–O and Si–N distances. Furthermore, the emission spectrum in Figure 10 indicates Eu^{2+} with mainly O coordination (see Luminescence Measurements).

The layers consist of dreier rings as shown in Figure 3. As all layers are oriented in the same way, a center of inversion

Table 2. Selected interatomic distances [pm] and angles [°] in $EuSi_2O_2N_2$ (standard deviation in brackets).

Eu1–O1	248(2)	Eu2–O3	250(2)	Eu3–O6	251(2)	Eu4–O2	247(3)
Eu1–O2	249(2)	Eu2–O4	250(2)	Eu3–O5	251(3)	Eu4–O7	250(2)
Eu1–O4	252(2)	Eu2–O8	253(2)	Eu3–O7	254(2)	Eu4–O1	251(2)
Eu1–O3	256(2)	Eu2–O6	254(2)	Eu3–O8	258(2)	Eu4–O5	257(3)
Eu1–O5	265(3)	Eu2–O1	266(3)	Eu3–O3	262(2)	Eu4–O8	264(3)
Eu1–O6	275(2)	Eu2–O7	266(2)	Eu3–O2	269(3)	Eu4–O4	274(2)
Eu1–N3	291(2)	Eu2–N8	280(2)	Eu3–N7	283(2)	Eu4–N1	293(2)
Si1–O2	162(3)	Si2–O1	159(2)	Si3–O4	162(2)	Si4–O3	163(2)
Si1–N2	171(2)	Si2–N3	172(2)	Si3–N5	173(2)	Si4–N6	174(2)
Si1–N1	172(2)	Si2–N8	172(2)	Si3–N1	174(2)	Si4–N4	174(2)
Si1–N7	174(2)	Si2–N1	175(2)	Si3–N6	177(2)	Si4–N3	175(2)
Si5–O5	158(3)	Si6–O6	159(2)	Si7–O8	163(3)	Si8–O7	161(2)
Si5–N5	171(2)	Si6–N6	173(2)	Si7–N4	172(2)	Si8–N4	174(2)
Si5–N3	175(2)	Si6–N8	175(2)	Si7–N7	174(2)	Si8–N2	174(2)
Si5–N7	175(2)	Si6–N2	176(2)	Si7–N8	176(2)	Si8–N5	175(2)
Si2-N1-Si3	113.7(8)	Si1-N2-Si8	115.8(8)	Si2-N3-Si4	115.9(8)		
Si1-N1-Si2	120.6(8)	Si1-N2-Si6	118.6(8)	Si4-N3-Si5	118.5(8)		
Si1-N1-Si3	122.1(8)	Si6-N2-Si8	120.0(8)	Si2-N3-Si5	121.5(8)		
Si4-N4-Si8	116.6(7)	Si3-N5-Si5	115.4(7)	Si3-N6-Si6	118.0(7)		
Si7-N4-Si8	117.8(8)	Si3-N5-Si8	118.8(7)	Si4-N6-Si6	118.1(8)		
Si4-N4-Si7	119.4(7)	Si5-N5-Si8	122.5(8)	Si3-N6-Si4	119.2(7)		
Si1-N7-Si5	115.7(7)	Si6-N8-Si7	116.2(7)				
Si5-N7-Si7	118.3(7)	Si2-N8-Si7	119.1(7)				
Si1-N7-Si7	121.3(7)	Si2-N8-Si6	119.6(7)				

is clearly absent in the structure. Layers with the same up-down scheme of terminal O atoms are present in sinoite,[8] however, in that mineral these O atoms directly connect consecutive layers to form a dense framework. In $EuSi_2O_2N_2$ the layers are interconnected through Eu^{2+} ions

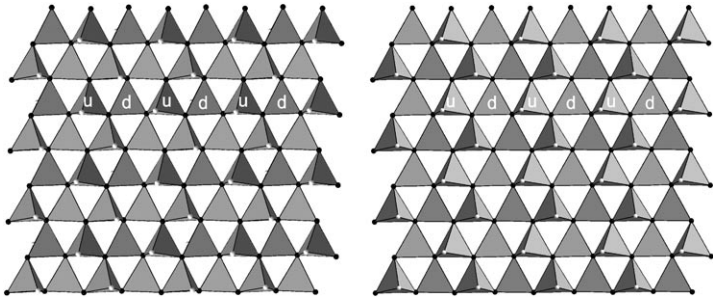

Figure 3. Comparison of the $Si_2O_2N_2^{2-}$ layers in $EuSi_2O_2N_2$ (left; view along [110]) and in Si_2N_2O (right; view along [011]); O white, N black. "u" and "d" represent the orientation of the tetrahedron vertices ("*u*p" and "*d*own").

that form distorted hexagonal layers (Figure 4a). The complete Eu substructure can be described with a smaller centrosymmetric unit cell. The silicate layers also exhibit pseudotranslational symmetry (cf. Figure 4a), however, the combination of both can only be described with the larger triclinic unit cell given above, resulting in *P*1 as the only possible space group.

Figure 4b illustrates why twinning is likely: The O atoms of one silicate layer that coordinate Eu atoms form distorted planar square nets that adopt a similar position after a 180° rotation around the [010]* direction which is perpendicular to the layers. Thus, a rotated layer can bond to Eu in the same way as the original one.

The Eu atoms are coordinated by six O atoms, leading to a distorted trigonal prism, which is capped by one N atom (Figure 5). All interatomic distances are within the typical range, some are given in Table 2.

High-resolution electron microscopy (HRTEM): HRTEM images with various zone axes and defocus values agree well with image simulations based on the structure model derived from X-ray data. However, some crystallites clearly exhibit stacking faults and/or twin boundaries. Figure 6 shows one of them (two different defocus values) and demonstrates that images can easily be correlated with structure projections. Image simulations are inserted in an "ideal" part of the crystallite. The boundary shown involves a shift between the two parts by *c*/4, which can be explained by a movement of the pseudohexagonal Eu layer,

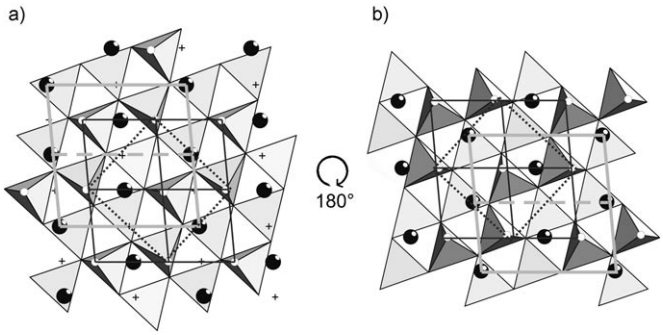

Figure 4. Layers in $EuSi_2O_2N_2$, view along [010]*: a) Representation of one silicate layer (the smallest repeating unit is indicated by a dotted line) and the following Eu layer (pseudohexagonal net of black spheres); the unit cell is indicated by gray lines, the pseudotranslation in the Eu net is indicated by a broken line. The crosses indicate alternative Eu positions (see text). b) A rotation of 180° in the drawing plane results in a similar atom arrangement. The O atoms form a distorted square net (black lines, also shown in a)), which has a similar orientation after the rotation of the silicate layer (NB: the silicate layer itself has a different orientation).

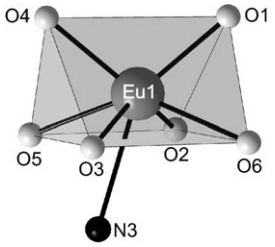

Figure 5. Coordination sphere of the Eu1 ion. The four crystallographically different Eu sites in $EuSi_2O_2N_2$ exhibit nearly the same surrounding (as proved by Mössbauer spectroscopy).

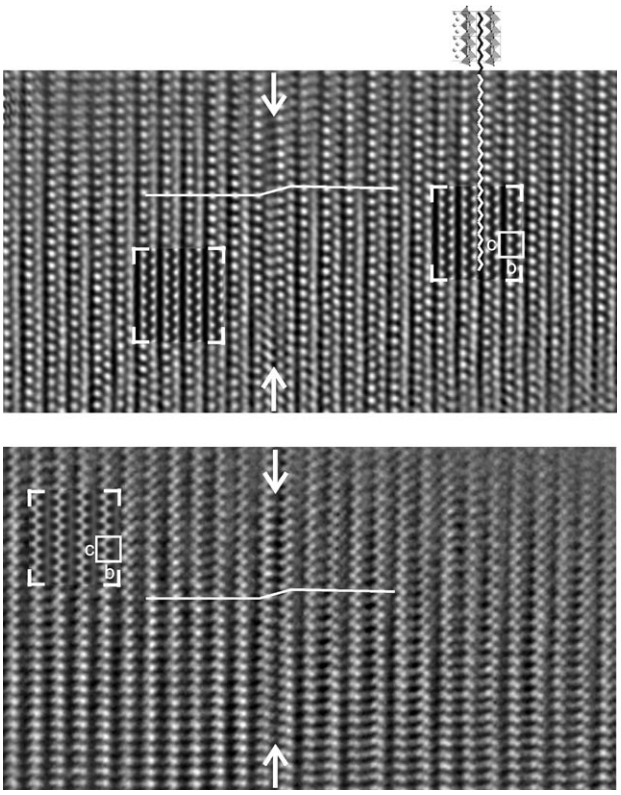

Figure 6. High-resolution images of a $EuSi_2O_2N_2$ crystallite, zone axis [100]. The arrows indicate the twin boundary, the insets show image simulations (multi-slice formalism, $t=2.8$ nm, top: $\Delta f=-35$ nm, bottom: $\Delta f=+5$ nm). The zigzag line highlights the position of the Eu atoms, illustrated by the structure image (top right). The image was taken from a wedge-shaped crystallite edge (increasing thickness), so that the simulations fit well for a small area only.

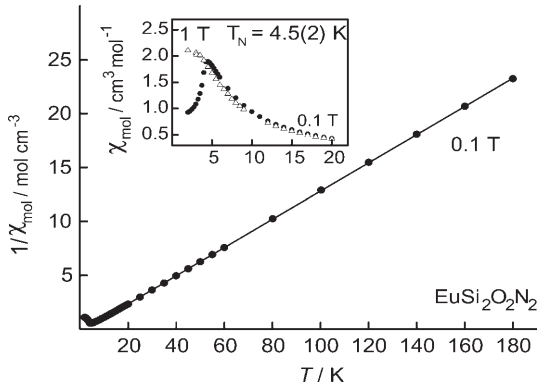

Figure 7. Temperature dependence of the inverse magnetic susceptibility of $EuSi_2O_2N_2$ measured at 0.1 T. The low-temperature behavior is shown in the inset.

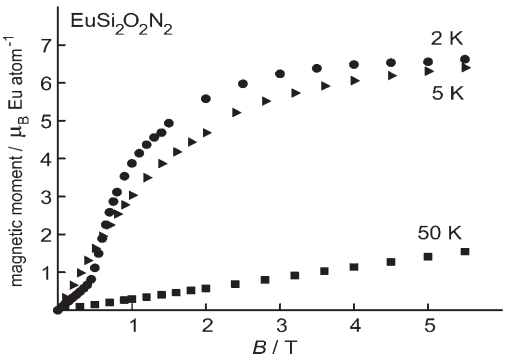

Figure 8. Magnetization versus external field strength of $EuSi_2O_2N_2$ measured at 2, 5, and 50 K.

which adopts a similar position with respect to the silicate layer after this shift as shown by crosses in Figure 4a. As the silicate layer can adopt the position obtained after the 180° rotation discussed above, imperfections like this can be twin boundaries as well as antiphase domain boundaries.

Magnetic properties: In Figure 7 the temperature dependence of the inverse magnetic susceptibility of $EuSi_2O_2N_2$ is presented as measured at magnetic flux densities of 0.1 T. Above 20 K Curie–Weiss behavior is observed, $\chi=C/(T-\Theta)$ with an experimental magnetic moment of 7.80(5) $\mu_B\,Eu^{-1}$, close to the free ion value of 7.94 μ_B for Eu^{2+}. The paramagnetic Curie temperature of $\Theta=2.2(2)$ K was determined by linear extrapolation of the $1/\chi$ versus T data to $1/\chi=0$. The positive paramagnetic Curie temperature is indicative of predominantly ferromagnetic interactions.

In the measurement at 0.1 T, magnetic ordering of the europium magnetic moments is detected at 4.5(2) K (see Figure 7 inset). At first sight this may be indicative of antiferromagnetism; however, already at a flux density of 1 T the Néel point disappears (Figure 7 insert). We have subsequently measured the magnetization behavior at 2, 5, and 50 K (Figure 8). At 50 K a linear increase of the magnetization is observed, as expected for a paramagnetic material. At 5 K, slightly above the magnetic ordering temperature, the increase is much steeper and the spin alignment continuously turns to a parallel alignment. At 2 K a field-induced (spin flip or metamagnetism) transition with a critical field of 0.50(5) T occurs. At 2 K and 5.5 T the magnetic moment is 6.62(5) $\mu_B\,Eu^{-1}$ atom, somewhat smaller than the theoretical value of 7.0 $\mu_B\,Eu^{-1}$ atom according to $g\times S$.[11] Thus, we have not reached a full parallel spin alignment. The paramagnetic moment and the saturation magnetization at low temperatures are comparable to the recently determined values for the nitridosilicate $Eu_2Si_5N_8$.[12]

The slightly too small magnetization at 2 K and 5.5 T as well as the positive paramagnetic Curie temperature (concurrence of antiferromagnetic and ferromagnetic interactions), the triangular europium arrangement, and structural disorder might also indicate spin glass behavior.

^{151}Eu Mössbauer spectroscopy: The ^{151}Eu Mössbauer spectrum of $EuSi_2O_2N_2$ recorded at 78 K is presented in Figure 9. A transmission integral fit was obtained by using the Levenberg–Marquard algorithm. The $EuSi_2O_2N_2$ structure has four crystallographically different europium sites, however, a superposition of their very similar Mössbauer

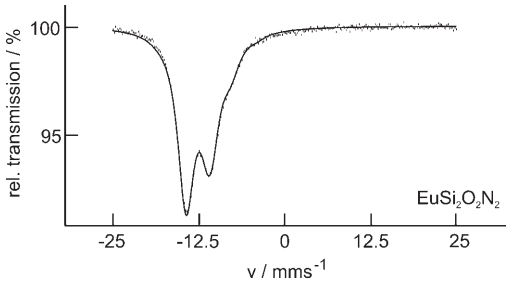

Figure 9. Experimental and simulated ^{151}Eu Mössbauer spectrum of $EuSi_2O_2N_2$ at 78 K.

signals is observed in the spectrum. At 78 K it could be well reproduced by a single europium site at an isomer shift of $\delta = -12.3(1)\ mm\,s^{-1}$, subject to quadrupole splitting of $\Delta E_Q = -2.3(1)\ mm\,s^{-1}$. The experimental line width is $\Gamma = 3.0(2)\ mm\,s^{-1}$. An asymmetry parameter $\eta = 0.46(3)$ was included in the fit. The latter most likely accounts for the unresolved difference of the electronic state of the four europium sites. The quadrupole splitting reflects the low site symmetry of the europium positions.

In excellent agreement with the magnetic data discussed above, no Eu^{III} impurity is detected in the ^{151}Eu Mössbauer spectrum. The isomer shift of $EuSi_2O_2N_2$ is slightly greater than that of $Eu_2Si_5N_8$ ($-11.82(5)\ mm\,s^{-1}$),[12] indicating a higher ionicity for $EuSi_2O_2N_2$.

The sample has further been measured at 4.2 K, slightly below the Néel temperature. Here, we observed only a small line broadening, which resulted from a small hyperfine field of 1.5(5) T at the europium nuclei. We expect stronger hyperfine field splitting at lower temperatures, however, our setup is limited to 4.2 K.

Luminescence measurements: To verify the luminescence properties of $EuSi_2O_2N_2$, excitation and emission spectra were recorded at room temperature. Owing to the similarity of the coordination of the four crystallographically different Eu sites, Figure 10 only shows a broad emission band peaking at $\lambda = 575$ nm (excitation wavelength $\lambda_{exc} = 450$ nm), which is characteristic for Eu^{2+} 5d→4f luminescence. No significant change of emission band shape for shorter wavelength excitation could be detected, which also reflects the chemical similarity of the different Eu sites. As expected from the Mössbauer measurement results, no line emission indicating Eu^{III} was observed for UV excitation.

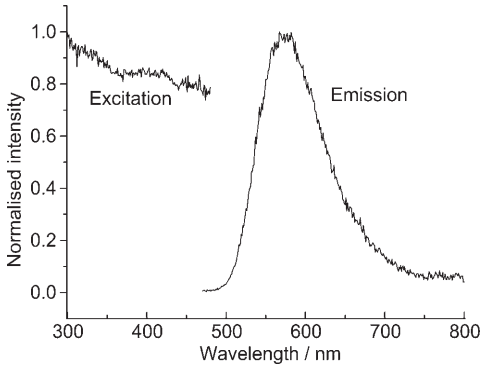

Figure 10. Excitation and emission spectra of $EuSi_2O_2N_2$.

At higher temperatures $EuSi_2O_2N_2$ shows thermochromy, which means that the samples′ color changes from yellow (25 °C) to deep orange at 500 °C. This phenomenon is accompanied by a reduction of the luminescence intensity with increasing temperature (*thermal quenching*). Owing to the high Eu^{II} luminescence center concentration of the title compound, the temperature-induced luminescence quenching is very pronounced due to concentration quenching. Figure 11 presents emission spectra at different temperatures.

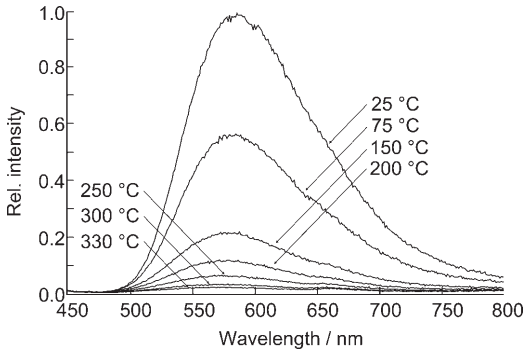

Figure 11. Emission spectra of $EuSi_2O_2N_2$ at different temperatures.

Conclusion and Future Prospects

The crystal structure of the new layered oxonitridosilicate $EuSi_2O_2N_2$ was obtained by a twin refinement and verified by HRTEM, magnetic, Mössbauer, and luminescence investigations. Pseudotranslational symmetry of parts of the structure (cf. Figure 4) gave rise to a number of real structure effects, such as twinning, antiphase domain boundaries, and coherently intergrown domains with different orientations. These phenomena appeared in numerous HRTEM investigations.

The oxidation state +II for all Eu ions in $EuSi_2O_2N_2$ has been confirmed by ^{151}Eu Mössbauer spectroscopy and magnetic measurements down to a temperature of 2 K. Also the emission spectra only show a broad band with a maximum at $\lambda = 575$ nm, which indicates 5d→4f luminescence of Eu^{II}. Eu^{3+} line emission was not observed.

Currently, we are conducting further investigations on the apparently very similar compound $SrSi_2O_2N_2$. This material is a promising phosphor for application in luminescence-conversion LEDs when doped with Eu^{2+}. The Sr analogue also seems to exhibit real structure effects that will be analyzed by HRTEM analyses. The aim is to achieve a complete characterization of these important substances.

Experimental Section

Single-crystal X-ray data were collected on a STOE IPDS diffractometer ($Mo_{K\alpha}$ radiation). The program package SHELX97 was used for structure solution and refinement.[13] Further details of the crystal structure investigation(s) may be obtained from the Fachinformationszentrum Karlsruhe, 76344 Eggenstein-Leopoldshafen, Germany (fax: (+49)7247–808–666; e-mail: crysdata@fiz-karlsruhe.de) on quoting the depository number CSD-416046.

Powder diffraction data were collected on a STOE STADI P diffractometer ($Mo_{K\alpha_1}$ radiation).

Electron diffraction patterns (SAD, selected area diffraction) and high-resolution images were recorded on a transmission electron microscope (Philips, model CM30/ST). The acceleration voltage was 300 kV, the spherical aberration constant C_s of the device was 1.15 mm, and the point resolution was 0.19 nm. Samples were finely ground and images were taken from thin regions near crystallite edges. The analysis and interpretation of the diffraction images and the computation of simulations were conducted by using the EMS program package.[14]

The magnetic susceptibilities of a polycrystalline, powdered sample of $EuSi_2O_2N_2$ were determined with a MPMS SQUID magnetometer (Quantum Design) in the temperature range 2 to 300 K with magnetic flux densities up to 5.5 T. A quantity of 5.058 mg was enclosed in a small silica tube and fixed at the sample holder rod. The sample was then cooled to 2 K in a zero magnetic field and slowly heated to room temperature in an applied external field.

The 21.53-keV transition of ^{151}Eu with an activity of 130 MBq (2% of the total activity of a $^{151}Sm:EuF_3$ source) was used for the Mössbauer spectroscopy experiments. The measurements were performed with a commercial helium bath cryostat. The temperature of the absorber could be varied from 4.2 to 300 K and was measured with a metallic resistance thermometer with a precision better than ± 0.5 K. The source was kept at room temperature. The material for the Mössbauer spectroscopy investigation was the same as for the susceptibility measurements. The sample was diluted with sugar and placed within a thin-walled PVC container at a thickness corresponding to about 10 mg Eu cm^{-2}.

Excitation and emission spectra were measured for powdered samples of $EuSi_2O_2N_2$ by means of an in-house built spectrometer system equipped with a 150-W Xe lamp, a 2× 500 mm Czerny Turner monochromator, 1800 L mm^{-1} gratings, 250/500 nm blaze, and a SPC multiplier detection unit. Temperature-dependent emission spectra were measured with an Edinburgh Inst. FS900 based spectrometer system equipped with a 450-W Xe lamp, a PMT based SPC detection unit with Peltier cooling, and an ohmic heater extension.

Synthesis of $EuSi_2O_2N_2$: In a typical experiment Eu_2O_3 (0.5 mmol, 176.0 mg; powder, Rhodia Electronics & Catalysis, La Rochelle, 99.99%) and silicon diimide (2.0 mmol, 116.3 mg; synthesized according to reference [15]) were placed in a tungsten crucible under an argon atmosphere inside a glove box (Unilab, MBraun, Garching, $O_2 < 0.1$ ppm, $H_2O <$ 0.1 ppm). Then the crucible was heated inductively in the reactor of a radio-frequency furnace[6] under a N_2 atmosphere (dried over silica gel/KOH/molecular sieve (pore width 4 Å)/P_2O_5 and activated BTS catalyst) to 1000 °C at a rate of about 33 °C min^{-1} and then kept at this temperature for 25 min. Subsequently, the temperature was increased to 1400 °C over 40 h. The reaction product was then cooled to 1200 °C in about 45 h and quenched to room temperature by switching off the furnace. A yellow, microcrystalline product was obtained, which was single-phase $EuSi_2O_2N_2$ according to the X-ray powder pattern. The elemental analysis (ICP-AES for Eu and Si; LECO TC-400 Analyzer for O and N, Philips Centre for Technology, Eindhoven) confirmed the expected sum formula: $EuSi_2O_2N_2$; 268.16 amu; Eu 55.3 (calcd 56.7), Si 21.1 (20.9), O 11.5 (11.9), N 12.4 (10.5) wt%.

Acknowledgements

This work was financially supported by the Fonds der Chemischen Industrie and by the Deutsche Forschungsgemeinschaft.

[1] H. Huppertz, W. Schnick, *Z. Anorg. Allg. Chem.* **1997**, *623*, 212–217.
[2] H. Huppertz, W. Schnick, *Chem. Eur. J.* **1997**, *3*, 249–252.
[3] H. Yamane, F. J. DiSalvo, *J. Alloys Compd.* **1996**, *240*, 33–36.
[4] H. A. Höppe, F. Stadler, O. Oeckler, W. Schnick, *Angew. Chem.* **2004**, *116*, 5656–5659; *Angew. Chem. Int. Ed.* **2004**, *43*, 5540–5542.
[5] R. Mueller-Mach, G. Mueller, M. R. Krames, H. A. Höppe, F. Stadler, W. Schnick, T. Juestel, P. Schmidt, *Phys. Status Solidi A* **2005**, *202*, 1727–1732.
[6] W. Schnick, H. Huppertz, R. Lauterbach, *J. Mater. Chem.* **1999**, *9*, 289–296.
[7] F. Stadler, *Diploma thesis*, University of Munich, **2003**.
[8] a) J. Sjoeberg, G. Helgesson, I. Idrestedt, *Acta Crystallogr. Sect. C* **1991**, *47*, 2438–2441; b) A. Bischoff, T. Grund. T. Jording, B. Heying, R.-D. Hoffmann, U. C. Rodewald, R. Pöttgen, *Z. Naturforsch. B*, **2005**, *60*, 1231–1234.
[9] F. Stadler, W. Schnick, unpublished results.
[10] H. Mattausch, O. Oeckler, R. K. Kremer, A. Simon, *Z. Anorg. Allg. Chem.* **2000**, *626*, 518–523.
[11] H. Lueken, *Magnetochemie*, Teubner, Stuttgart, **1999**.
[12] H. A. Höppe, H. Trill, B. D. Mosel, H. Eckert, G. Kotzyba, R. Pöttgen, W. Schnick, *J. Phys. Chem. Solids* **2002**, *63*, 853–859.
[13] G. M. Sheldrick, SHELX97, *Program package for the solution and refinement of crystal structures*, Release 97–2, University of Göttingen, Germany, **1997**.
[14] P. Stadelmann, *Ultramicroscopy* **1987**, *21*, 131–145.
[15] H. Lange, G. Wötting, G. Winter, *Angew. Chem.* **1991**, *103*, 1606–1625; *Angew. Chem. Int. Ed. Engl.* **1991**, *30*, 1579–1597.

Received: March 23, 2006
Published online: July 3, 2006

